COBEM 2021 26th International Congress of Mechanical Engineering
ABCM Associação Brasileira de Engenharia e Ciências Mecânicas
November 22-26, 2021, Virtual Congress, Brazil

COB-2021-1923 ANALYSIS OF COPPER ADDITION BY ELECTROLYSIS ON THE MICROSTRUCTURE AND CORROSION RESISTANCE OF LASER WELDED SUPER-DUPLEX STAINLESS STEEL

Bruna Berbel Seloto
Eli Cruz Junior
Leonardo Viela de Menezes Carvalho
Vicente Afonso Ventrella
Department of Mechanical Engineering, São Paulo State University
b.seloto@unesp.br; dacruz.eli@gmail.com;leonardo.vilela@unesp.br; vicente.ventrella@unesp.br

Abstract. *Duplex and super-duplex stainless steels receive this denomination due to their microstructure composed of austenite and ferrite, which contributes to good mechanical resistance and corrosion, however, subjecting them to the welding process, results in a weld bead with a predominantly ferritic structure, with distinct properties of the base metal. Thus, Nd:YAG pulsed laser welding presents a good alternative for these materials, since it offers low heat input, with energy density in weld bead, and, consequently, small heat affected zone. Even though this process presents good quality in the welding of super-duplex stainless steels, the unbalance of phases in fusion zone is still present. Some alloying elements act as austenite stabilizers , such as copper. Thus, the present work sought to add this element by electrodeposition with a time of 60, 80 and 100 minutes, current density 2 A/dm2, temperature of 50 ºC, and pH 1.0, with the use of an acidic solution of $CuSO_4$ in plates of 3 mm thick UNS S32750 super-duplex stainless steel. Subsequently, they were welded with an Nd:YAG pulsed laser welding process with the following fixed parameters: welding speed 1 mm/s, peak time 5 ms, frequency 9 Hz, pulse energy 10 J, peak power 2 kW, and argon shielding gas with a flow rate of 20 L/min. The analysis of the effects of copper addition occurred through the evaluation of microstructure, microhardness, and Potentiodynamic Polarization on the weld bead. The results demonstrate that copper deposition formed a uniform, adherent orange-colored coating. The macrographic and micrographic images indicate that there was an austenite formation mainly in grain boundaries, insoluble copper islands, cracks along the weld bead, and porosity. Regarding corrosion, among all the analyzed samples, there was no significant disparity difference in general corrosion but the Cu100 sample showed greater resistance to pitting corrosion.*

Keywords: *Nd:YAG pulsed laser welding, Super-duplex Stainless Steel, Copper Addition*

1. INTRODUCTION

The super duplex stainless steels there are high mechanical strength and corrosion resistance, these factors are due to the microstructure that is roughly half ferrite (δ) and half austenite (α) (Elsaady *et al.*, 2018). In this way, these steels are currently used for applications in environments with extreme conditions, for instance, pipelines, chemical storage tanks in cellulose plants and the construction of underwater components of offshore structures. Despite the good qualities of the material, when welding it with conventional welding processes, e.g., gas tungsten arc welding and friction stir welding, there are a promoting of ferrite phase in the microstructure and precipitate formation as Sigma phase, Chi and 'R' (Pramanik *et al.*, 2015).

Laser welding has some advantages over the other processes mentioned, such as ease of automation, small Heat-Affected Zone (HAZ), unbelievably short cycle time, and lower heat input (Sivakumar *et al.*, 2017). The high cooling rate of this process allows for a smaller amount of precipitates, however, the lack of time to transform the ferrite into austenite results in the imbalance of the phases (Silva Leite *et al.*, 2019).

In this way, some works tried to found control the ratio of austenite and ferrite in the weld beam on the duplex and super duplex stainless steel. Pramanik *et al.* (2015), have found that the control of welding velocity and adjusting the heat of laser is can improve the rate with austenite and ferrite about 15 percentage.Babu *et al.* (2019) studied the influence of heat dissipation on the formation of austenite and ferrite in the Nd: YAG pulsed laser welding by varying the cooling medium - air and oil - the latter increases the ferrite content in the weld bead.Pekkarinen and Kujanpää (2010) noted that duplex stainless steels depend on the cooling speed, control of laser welding parameters and chemical composition of the material.Silva Leite *et al.* (2019) welded using the Nd: YAG pulsed laser the dissimilar materials AISI 316L with super duplex UNS S32750 (SDSS), the results indicated that the amount of nickel in the AISI 316L influenced the appearance of a balanced ferrite and austenite bead. Finally, da Cruz Junior *et al.* (2021) added nickel sheets 30 µm thick when

laser welding Nd: YAG pulsed on UNS S32750 super duplex steel resulting in a weld bead close to 50% ferrite and 50% austenite.

Then, besides the welding parameters of the laser process, the nickel gamma elements also help the stability between ferrite and austenite. According to Lippold *et al.* (2015), some elements added in stain steels can promote austenite phase, viz., Nickel, Manganese, Carbon, Nitrogen, Copper, and Cobalt. An alternative to adding this material to the weld bead is through electrolysis, since the amount of material needed in this process is small, making laser welding easier. So, the objective of this work is to add copper in UNS S32750 super duplex stain steel sheets through electrodeposition and then welding this with Nd: YAG pulsed laser welding to improve the volume fraction of austenite.

2. MATERIALS AND METHODS

The base metal used was the UNS S32750 in sheets 1.5 mm thick, cut by Electrical Discharge Machining (EDM) resulting in the final dimensions 30x12.5x1.5 mm the material's chemical composition is reported in Tab. 1.

Table 1: Chemical composition of UNS S32750.

Metal Base	%C	%Si	%Mn	%Cr	%Ni	%Mo	%S	%P	%N
UNS S 32750	0,018	0,29	0,63	25,61	6,97	3,84	0,003	0,022	0,269

Fonte:Realum.

After cutting, clean the material is important to ensure adhesion. So, the sheets were sanded with 1500 weight sandpaper, next they were submerged in the 200 g/L NaOH ultrasonic bath for 5 minutes and, and then dry. This alkaline degreasing is essential since the cutting equipment Electrical Discharge Machine uses an oil-contaminated cooling fluid. After that, using electrolysis, copper covered the samples up to a height of 9.6 mm, so the total area covered was 960 mm² in all samples, how shown Fig. 1.

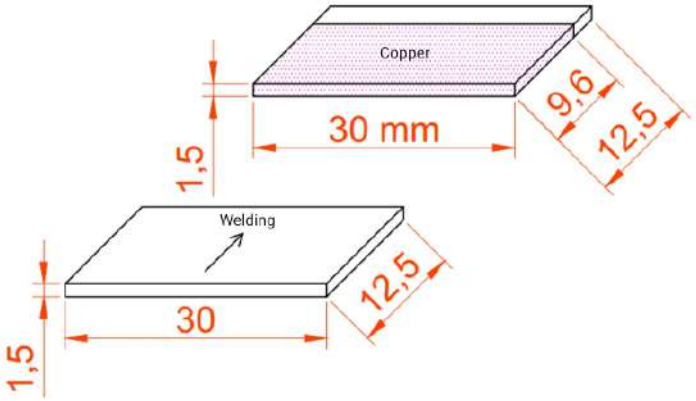

Figure 1: Schematic copper electrolysis

The solution used in this work was 10g of $CuS0_4.5H_2O$, 4 ml of H_2SO_4 dissolved in 200 ml of H_20 at a temperature of 50 ºC, and current density of 2 A/dm², based on the literature of Panda (2017). The time for each electrolytic bath was the result of trial and error.

After each electrolysis, the layer thickness was measured using an external digital micrometer (293-230 Mitutoyo) at ten different points to calculate the mean and standard deviation. Each measure was divided by two because both sides of the sheets were covered by copper.

Finally, the sheets were weld with Nd: YAG pulsed laser machine model UW-150A, with a 150 W maximum power. The parameters remained fixed only by varying the time and thickness of copper deposition. Tab. 2 below shows the welding parameters. Each sample analyzed by the Stereo Microscope Zeiss - Discovery V8 to get the macrograph of the weld beads.

After the welding process, the samples were sectioned in the cross-section of the laser welding joint and then polished and etched using modified Behara (20 ml de HCl, 80 ml H_2O, 1 g de $K_2S_2O_5$, 2 g de NH_4HF_2) for the macroscopic examination using the Carls Zeiss -Neophoto 21 microscope to verifying the amount of austenite. The objective was around 50 % austenite.

The Vickers microhardness test was performed on the entire weld beam, using a 100 gf load for 10s at an interval of 0.08 mm respecting the ASTM-E384 standard, which establishes a minimum distance of 2.5 times the diameter of the indentation. To characterize the corrosive behavior of welded metal and base metal, the VoltaLab device, model PGZ 402, and Voltamaster 4 software performed the potentiodynamic polarization test. This equipment has an electrochemical

cell with 3 electrodes - the work, reference, and auxiliary. The test used a scanning speed of 1 mV/s and an electrolyte of seawater from Guaruja - Brazil with a pH of 7.05. The polarization curve was obtained according to ASTM-G3 and ASTM-G5. In these experiments, corrosion tests with each specimen were conducted minimum three times for reproducibility.

Table 2: Welding parameters for experiments.

Welding parameters	**Established values**
Peak Power	2.00 kW
Shield Gas	20 L/min
Welding speed	1.00 mm/s
Pulse Span	5.00 ms
Pulse Energy	10.00 J
Frequency	9.00 Hz

3. Results and Discussion

3.1 Macro and Microstructures of the Welded Joint

Altogether, three Cu samples were produced, with 60, 80, and 100 minutes of deposition. After electrolysis, the thickness was measured with a micrometer. These values and their corresponding samples are given in Tab. 3.

Table 3: Copper electrolysis thickness

Sample's name	**Time (min)**	**Thickness (µm)**	**Standa deviation (µm)**
Cu60	60	38.70	5.06
Cu80	80	75.90	4.82
Cu100	100	163.10	46.86

Macroscopic analysis of the Cu weld beads shows that there was a crack in all extensions in the three samples. Note that Fig.2 shows the oxidized surface probably caused by the insufficiency of the argon shielding gas flow. Fig. 3 and Fig. 4 have no oxidation, with a clean and shiny weld beam.

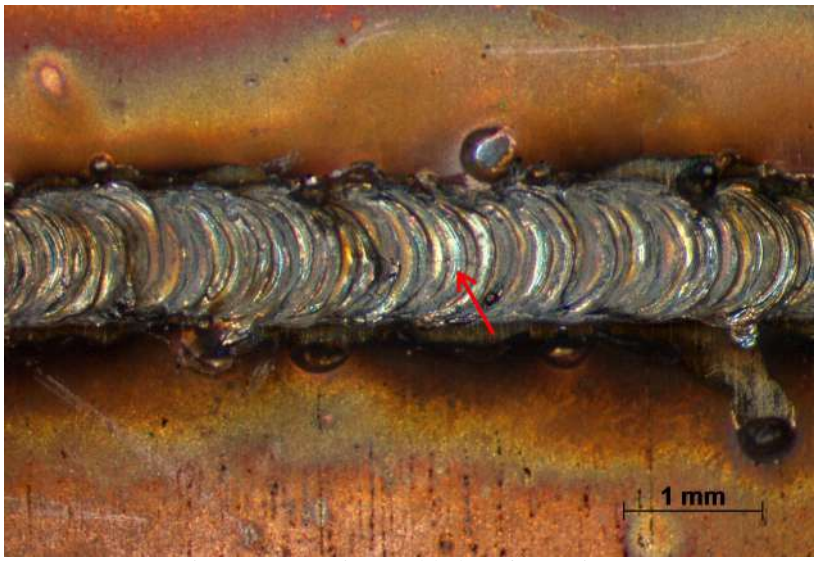

Figure 2: Top view welded Cu60 specimen.

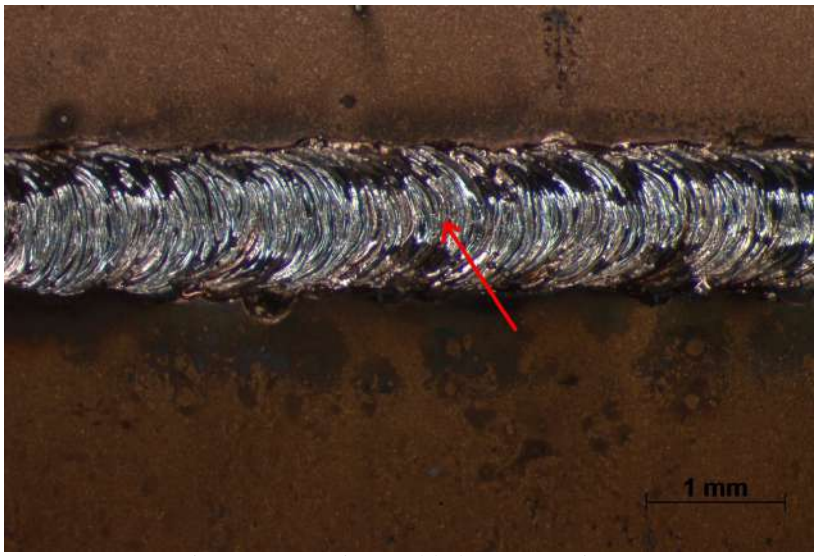

Figure 3: Top view welded Cu80 specimen.

Figure 4: Top view welded Cu100 specimen.

The Fig. 5a refers to Cu60, where copper "islands" are shown within the super duplex structure. This was observed in other studies. Chen *et al.* (2015) investigated the influence of processing parameters on steel/copper laser welding, the researchers identified spherical particles of copper with stainless steel because of liquid separation reactions induce. Kar *et al.* (2016) studied the electron beam welding between the dissimilar weld of Austenitic stainless steel 304L and copper, result shows that there were a large amount of porosity, cracks and copper globules.

The interface between Base Metal and fusion zone of the sample Cu100 is below in Fig. 5b where there are iron and copper separately, Chen *et al.* (2015) and Kar *et al.* (2016) reported very similar structure in their works. Moreover, in this region there are some irradiated microcracks. In both Fig. 5a and 5b is notable that copper, as well as stainless steel, are immiscible.

In welding with a high cooling rate, as laser welding, there is the formation of two fluids: iron-rich and copper-poor (Munitz, 1995). The copper-containing liquid agglutinates with other copper islands due to the large convection in the molten pool, but in some cases, the kinetic energy of these copper agglomerates is not enough to unite and form small copper mounds. Another relevant factor is that between both materials there are different Melting Points and different thermal conductivity coefficients, a factor that favors the formation of cracks. Therefore, the more copper then the more complicated the soldering becomes because of the formation of cracks. Because of this, the study has limited samples to up to 100 minutes, not only because of the that, but also because there is a limited focus on the laser machine. Thus, despite the formation of secondary austenite (Fig. 5b), there was no phase equilibrium around 50% austenite and 50% ferrite.

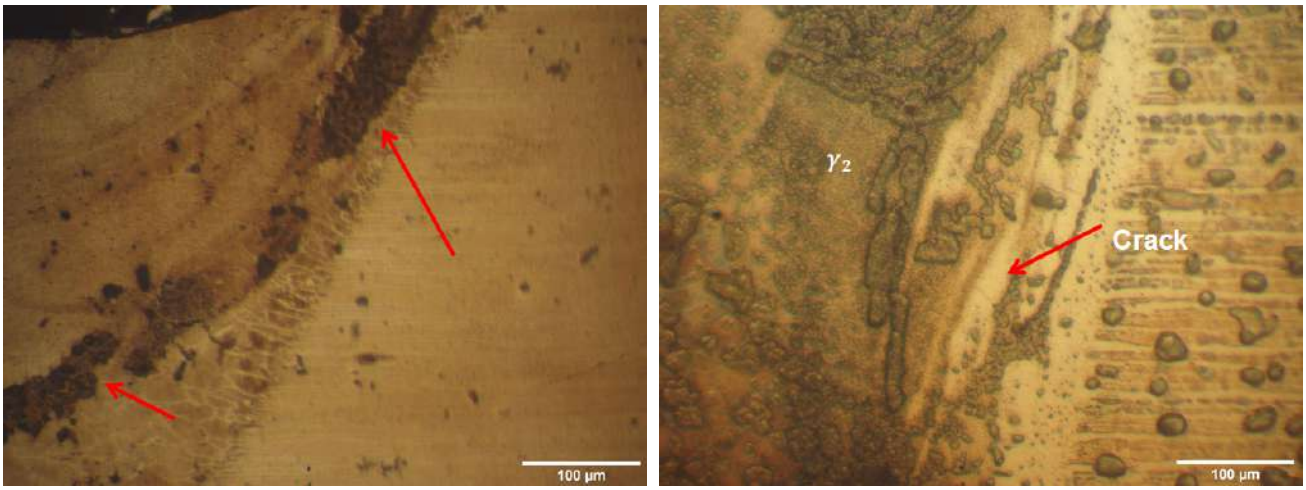

(a) Copper islands. (b) Crack and secondary austenite (γ_2).

Figure 5: Micrographs of Cu60 weld bead.

3.2 Microhardness

The graph in the Fig. 6 demonstrates the microhardness profile along the weld joint of the three samples: Cu60, Cu80, and Cu100. The hardness of the base metal remained practically constant, with an increase for the three specimens in the fusion zone. This factor is due to the amount of ferrite in the region, thus, because there are traces of secondary austenite, the hardness of the C100 sample is slightly lower among the other specimens. In the Cu100 weld, the microhardness value fluctuates rapidly at one point, the indentation probably occurred in one of the copper "islands" present in the bead. Copper has lower microhardness than iron (Chen *et al.*, 2015).

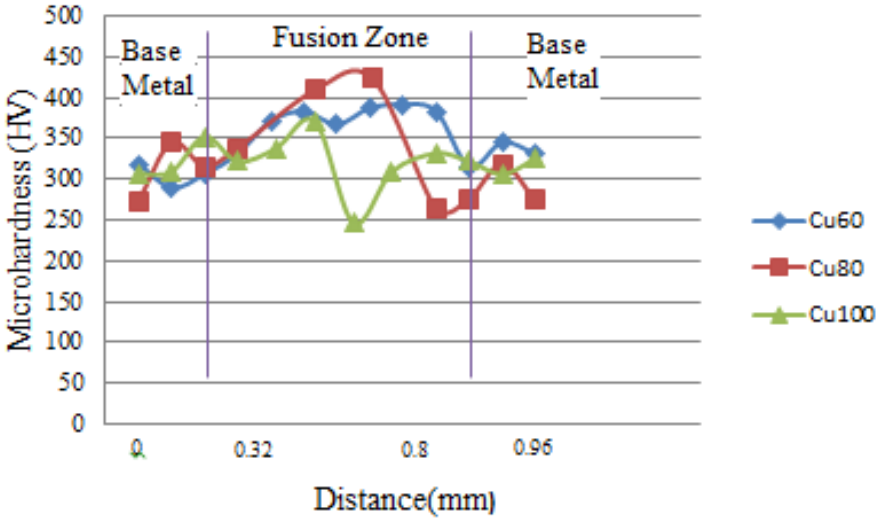

Figure 6: Microhardness profile along the weld beam.

3.3 Corrosion

The Fig.7 illustrates the results of the potentiodynamic polarization curve and the Tab. 4 summarizes the values of the Electrochemical Parameters from them. The test was performed on a 10 mm circumference in such a way that the weld bead and part of the base metal are covered. The graph shows, for comparison purposes, the curve of the UNS S32750 material without welding, calling it as "Base Metal".

Analyzing the graph, the Cu100 sample showed greater resistance to pitting corrosion than the other specimens, with a pitting potential of 1611 mV (Tab. 4). Cu80 showed the lowest value of all, 790 mV. It can be observed that in terms of general corrosion, there is no significant difference for the samples analyzed, with corrosion potential values close to each other.

Although secondary austenite is not as resistant to pitting corrosion as primary austenite (Nilsson *et al.*, 1995), this

phase may have increased the pitting potential of the Cu100 sample.

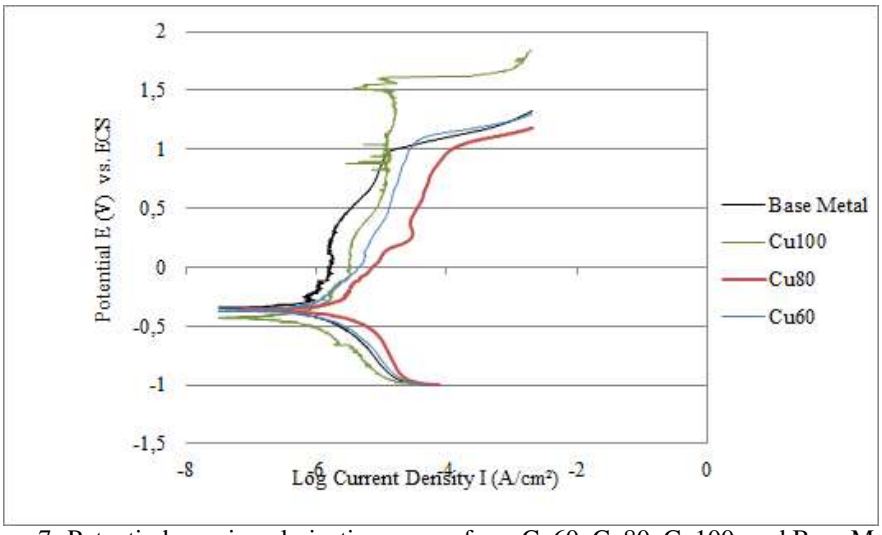

Figure 7: Potentiodynamic polarization curves from Cu60, Cu80, Cu100, and Base Metal.

Table 4: Corrosion resistance information.

Samples	Corrosion Potential (mV)	Pitting Potential (mV)
Cu60	-377.5 $\pm$ 25	1050 $\pm$ 55
Cu80	-361.1 $\pm$ 14	790 $\pm$ 61
Cu100	-437.0 $\pm$ 22	1611 $\pm$ 67
Base Metal	-357.8 $\pm$ 30	997 $\pm$ 12

Cu is usually added to ferritic, austenitic and duplex stainless steels to improve their corrosion resistance. Although, several factors besides the chemical composition influence the final result. The copper samples did not have good results in the quality of the weld, with a large number of cracks, so in this region, there is the most probability to have pitting. Fig. 8a, 8b, and 8c show, in red arrow, the places where there is pitting for Cu samples, they all happened on cracks.

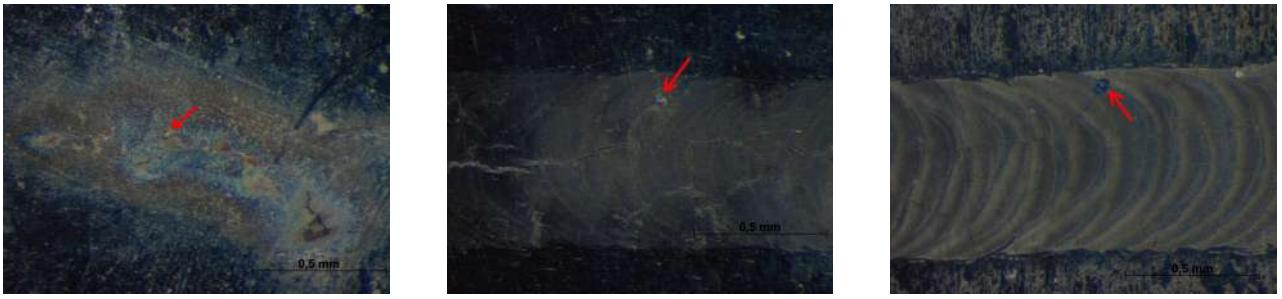

(a) (b) (c)

Figure 8: Images of corroded surfaces and pitting formation in (a) Cu60, (b) Cu80, and (c) Cu100.

3.4 Conclusion

The addition of copper gammagenic element through electrolysis in UNS S32750 super-duplex stainless steel for Nd:YAG pulsed laser welding allowed us to conclude that:

- The addition of copper results in the formation of cracks arising from the high coefficient of thermal conductivity in relation to the base metal.
- Copper agglomerates are formed due to the flow of the weld pool and the different coefficients of thermal conductivity of the materials, making them immiscible.
- Although copper did not form primary austenite, secondary austenite did form in the Cu100 bead.

- Even though in terms of general corrosion, there is no significant difference for the analyzed samples, the Cu100 specimen showed greater resistance to pitting corrosion than the others.
- The cracks favored the formation of pitting in this region.

4. ACKNOWLEDGEMENTS

National Council for Scientific and Technological Development (CNPq) for the financial support for this work.

5. REFERENCES

ASTM-E384, 2017. *SStandard Test Method for Microindentation Hardness of Materials*. ASTM International, West Conshohocken, PA.

ASTM-G3, 2019. *Standard Practice for Conventions Applicable to Electrochemical Measurements in Corrosion Testing*. ASTM International, West Conshohocken, PA.

ASTM-G5, 2021. *Standard Reference Test Method for Making Potentiodynamic Anodic Polarization Measurements*. ASTM International, West Conshohocken, PA.

Babu, P.D., Gouthaman, P. and Marimuthu, P., 2019. "Effect of heat sink and cooling mediums on ferrite austenite ratio and distortion in laser welding of duplex stainless steel 2205". *Chinese Journal of Mechanical Engineering*, Vol. 32, No. 1, pp. 1–9.

Chen, S., Huang, J., Xia, J., Zhao, X. and Lin, S., 2015. "Influence of processing parameters on the characteristics of stainless steel/copper laser welding". *Journal of Materials Processing Technology*, Vol. 222, pp. 43–51.

da Cruz Junior, E., Gallego, J., Settimi, A., Gennari, C., Zambon, A. and Ventrella, V., 2021. "Influence of nickel on the microstructure, mechanical properties, and corrosion resistance of laser-welded super-duplex stainless steel". *Journal of Materials Engineering and Performance*, Vol. 30, No. 4, pp. 3024–3032.

Elsaady, M.A., Khalifa, W., Nabil, M.A. and ElMahallawi, I.S., 2018. "Effect of prolonged temperature exposure on pitting corrosion of duplex stainless steel weld joints". *Ain Shams Engineering Journal*, Vol. 9, pp. 1407–1415.

Kar, J., Roy, S.K. and Roy, G.G., 2016. "Effect of beam oscillation on electron beam welding of copper with aisi-304 stainless steel". *Journal of Materials Processing Technology*, Vol. 233, pp. 174–185.

Lippold, J.C. *et al.*, 2015. *Welding metallurgy and weldability*. Wiley Online Library.

Munitz, A., 1995. "Metastable liquid phase separation in tungsten inert gas and electron beam copper/stainless-steel welds". *Journal of materials science*, Vol. 30, No. 11, pp. 2901–2910.

Nilsson, J.O., Karlsson, L. and Andersson, J.O., 1995. "Secondary austenite for mation and its relation to pitting corrosion in duplex stainless steel weld metal". *Materials Science and Technology*, Vol. 11, No. 3, pp. 276–283.

Panda, H., 2017. *Handbook on Electroplating with Manufacture of Electrochemicals: how to start electroplating industry in india, electrochemicals manufacturing industry in india, most profitable electrochemicals manufacturing business ideas, electroplating based profitable projects, electroplating processing projects, how to start an electrochemicals production business, electroplating based small scale industries projects, new small scale ideas in electroplating processing industry, npcs, niir, process technology books*. Asia Pacific Business Press Inc.

Pekkarinen, J. and Kujanpää, V., 2010. "The effects of laser welding parameters on the microstructure of ferritic and duplex stainless steels welds". *Physics Procedia*, Vol. 5, pp. 517–523.

Pramanik, A., Littlefair, G. and Basak, A., 2015. "Weldability of duplex stainless steel". *Materials and Manufacturing Processes*, Vol. 30, No. 9, pp. 1053–1068.

Silva Leite, C.G., da Cruz Junior, E.J., Lago, M., Zambon, A., Calliari, I. and Ventrella, V.A., 2019. "Nd: Yag pulsed laser dissimilar welding of uns s32750 duplex with 316l austenitic stainless steel". *Materials*, Vol. 12, No. 18, p. 2906.

Sivakumar, G., Saravanan, S. and Raghukandan, K., 2017. "Investigation of microstructure and mechanical properties of nd: Yag laser welded lean duplex stainless steel joints". *Optik*, Vol. 131, pp. 1–10.